ACS chemical biology

Articles

Cite This: ACS Chem. Biol. 2019, 14, 941−948

pubs.acs.org/acschemicalbiology

Biocatalytic Detoxification of Paralytic Shellfish Toxins

April L. Lukowski,[†,‡] Nicholas Denomme,[§,∥] Meagan E. Hinze,[‡] Sherwood Hall,[⊥] Lori L. Isom,[§,#,▽] and Alison R. H. Narayan*[,†,‡,○]

[†]Program in Chemical Biology and [‡]Life Sciences Institute, University of Michigan, Ann Arbor, Michigan 48109, United States

[§]Department of Pharmacology and [∥]Center for Consciousness Science, University of Michigan Medical School, Ann Arbor, Michigan 48109, United States

[⊥]United States Food and Drug Administration, College Park, Maryland 20740, United States

[#]Department of Neurology, [▽]Department of Molecular and Integrative Physiology, and [○]Department of Chemistry, University of Michigan, Ann Arbor, Michigan 48019, United States

Supporting Information

ABSTRACT: Small molecules that bind to voltage-gated sodium channels (VGSCs) are promising leads in the treatment of numerous neurodegenerative diseases and pain. Nature is a highly skilled medicinal chemist in this regard, designing potent VGSC ligands capable of binding to and blocking the channel, thereby offering compounds of potential therapeutic interest. Paralytic shellfish toxins (PSTs), produced by cyanobacteria and marine dinoflagellates, are examples of these naturally occurring small molecule VGSC blockers that can potentially be leveraged to solve human health concerns. Unfortunately, the remarkable potency of these natural products results in equally exceptional toxicity, presenting a significant challenge for the therapeutic application of these compounds. Identifying less potent analogs and convenient methods for accessing them therefore provides an attractive approach to developing molecules with enhanced therapeutic potential. Fortunately, Nature has evolved tools to modulate the toxicity of PSTs through selective hydroxylation, sulfation, and desulfation of the core scaffold. Here, we demonstrate the function of enzymes encoded in cyanobacterial PST biosynthetic gene clusters that have evolved specifically for the sulfation of highly functionalized PSTs, the substrate scope of these enzymes, and elucidate the biosynthetic route from saxitoxin to monosulfated gonyautoxins and disulfated C-toxins. Finally, the binding affinities of the nonsulfated, monosulfated, and disulfated products of these enzymatic reactions have been evaluated for VGSC binding affinity using mouse whole brain membrane preparations to provide an assessment of relative toxicity. These data demonstrate the unique detoxification effect of sulfotransferases in PST biosynthesis, providing a potential mechanism for the development of more attractive PST-derived therapeutic analogs.

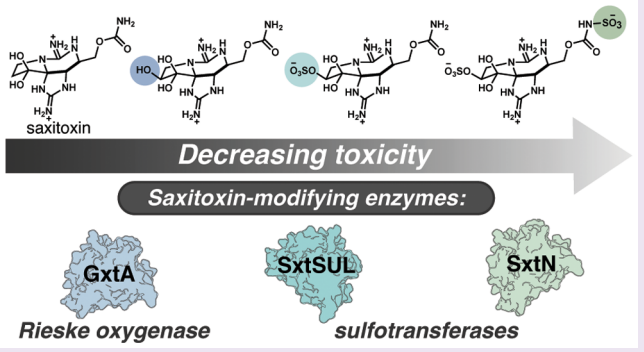

INTRODUCTION

Paralytic shellfish toxins (PSTs) are structurally complex small molecules with nanomolar affinity for tetrodotoxin-sensitive voltage-gated sodium channels (VGSCs).[1,2] PSTs share a common tricyclic, bisguanidinium ion-containing scaffold that is differentially functionalized at the C11, C12, N1, and C13 positions (Figure 1).[1,2] A subset of PSTs contain sulfate groups, including gonyautoxins (GTX1−6, **6**−**11**), C-toxins C1−C4 (**12**−**15**), and M-toxins M1α (**3**), M1β (**4**), and M3 (**5**).[2−4] Sulfated PSTs are often the most abundant species in mixtures of toxins isolated from biological sources.[5−7] While risk of systemic toxicity has hindered clinical studies with highly potent molecules from this class, such as saxitoxin (STX, **1**) and neosaxitoxin (neoSTX, **2**), PSTs bearing at least one sulfate group, such as GTX5 (**10**), have greater potential as safe pharmaceutical agents due to their reduced toxicity.[8,9] For example, gonyautoxins are being evaluated as agents for the treatment of pain and are currently in clinical trials for their ability to reduce acute pain in small doses (i.e., 40−50 μg injections). Importantly, these compounds elicit the desired analgesic effect without the possible cardiotoxicity and abuse potential observed with conventional local anesthetics. Specifically, GTX5 (**10**) and mixtures of GTX2 (**7**) and GTX3 (**8**) have been evaluated in clinical trials to treat chronic tension headaches,[10] muscle tension and spasms,[11,12] and postoperative pain associated with knee replacement surgery.[13] Botulinum toxin proteins have been extensively developed for these types of applications;[14] however, small molecule agents with similar capabilities possess significant advantages compared to protein therapeutics, including increased stability,

Received: February 14, 2019
Accepted: March 28, 2019
Published: April 15, 2019

DOI: 10.1021/acschembio.9b00123
ACS Chem. Biol. 2019, 14, 941−948

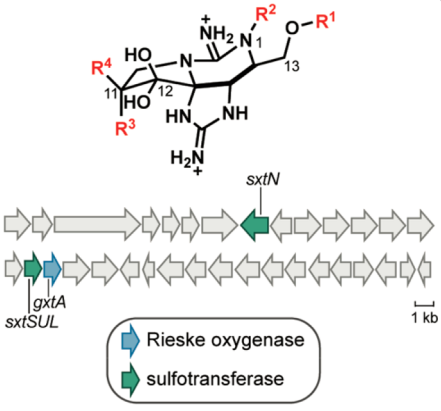

R^1	R^2	R^3	R^4	Name	Compound #
$CONH_2$	H	H	H	saxitoxin (STX)	1
$CONH_2$	OH	H	H	neosaxitoxin (neoSTX)	2
$CONH_2$	H	OH	H	M1α	3
$CONH_2$	H	H	OH	M1β	4
$CONH_2$	H	OH	OH	M3	5
$CONH_2$	OH	OSO_3^-	H	gonyautoxin 1 (GTX1)	6
$CONH_2$	H	OSO_3^-	H	gonyautoxin 2 (GTX2)	7
$CONH_2$	H	H	OSO_3^-	gonyautoxin 3 (GTX3)	8
$CONH_2$	OH	H	OSO_3^-	gonyautoxin 4 (GTX4)	9
$CONHSO_3^-$	H	H	H	gonyautoxin 5 (GTX5)	10
$CONHSO_3^-$	OH	H	H	gonyautoxin 6 (GTX6)	11
$CONHSO_3^-$	H	OSO_3^-	H	C1	12
$CONHSO_3^-$	H	H	OSO_3^-	C2	13
$CONHSO_3^-$	OH	OSO_3^-	H	C3	14
$CONHSO_3^-$	OH	H	OSO_3^-	C4	15

Reference	Assay type	System	Value reported	Relative potency
Genenah & Shimizu (1981)[46]	lethality	mouse	relative toxicity (ratio)	GTX2 < STX ≤ GTX3
Hall (1982)[47]	lethality	mouse	mouse units/μmol*	GTX2 < GTX3 ≈ STX
Strichartz *et al.* (1986)[48]	binding	rabbit brain	K_i	GTX2 < STX < GTX3
Kao *et al.* (1985)[45]	electrophysiological recording	squid axon	ED_{50}	GTX2 < GTX3 < STX
Usup *et al.* (2004)[42]	binding	rat brain	EC_{50}	GTX2/3 < STX
Alonso *et al.* (2014)[43]	electrophysiological recording	isolated channels	IC_{50}	GTX2/3 ≈ STX†
this study	binding	rat brain	K_i	GTX2/3 < STX

*Mouse units are defined as the amount of toxin required to kill a 20 g female mouse in 15 minutes via injection.
†Values were obtained for 7 VGSCs and the general trend is summarized.

Figure 1. Structures of select paralytic shellfish toxins and reported data on relative voltage-gated sodium channel affinity and toxicity for STX (**1**), GTX2 (**7**), and GTX3 (**8**).

milder storage conditions, longer shelf lives, and a wider range of dosing options.[15,16] Synthetic routes for accessing saxitoxin and gonyautoxins have been successfully developed,[17−20] though they typically require lengthy, inefficient routes or starting materials that are extracted from toxic shellfish.[10,21] Elucidating a biosynthetic route for producing sulfated PST derivatives stands to expedite production of these molecules and will enable structural diversification for the discovery of novel pharmaceutical agents and tools for fundamental biological studies.[22,23]

The toxification and detoxification of PSTs to modulate affinity for VGSCs have been employed by both prokaryotic[24,25] and eukaryotic organisms.[26,27] Typically, microorganisms responsible for the production of the sulfated PSTs are consumed by shellfish, which subsequently bioaccumulate the toxins and in some cases perform enzymatic modifications that alter the molecules' toxicity.[26,27] For example, it was recently reported that the marine scallop *Chlamys farreri* enzymatically hydrolyzes the sulfate groups of stored gonyautoxins to generate the more toxic parent compounds STX (**1**) and neoSTX (**2**), weaponizing the accumulated toxins for self-defense.[28] *C. farreri* possess point mutations in VGSC genes that reduce the affinity of PSTs for the channels, enabling the sequestration of up to 40,000 μg STX (**1**) per 100 g flesh, a quantity 500 times higher than the safety limit issued by the United States Food and Drug Administration and many other countries.[28−30] This extraordinary adaptation has motivated our research into the mechanisms of sulfotransferase-mediated modification of PSTs by the microorganisms responsible for their production.

Despite the abundance of sulfated derivatives isolated from natural sources,[7,31] the order of events in the biosynthetic route to singly sulfated derivatives (GTX1−6 and M-toxins) and disulfated PSTs (C-toxins 1−4) has not been elucidated and the biocatalytic machinery has remained uncharacterized. Our work is informed by initial *in vitro* studies using enzymes isolated from PST-producing dinoflagellate cultures performed by Ishida and co-workers, which provided evidence for the involvement of two sulfotransferases of unknown sequence in gonyautoxin biosynthesis: one capable of *N*-sulfamation of the C13 carbamate to afford GTX5 (**10**) from STX (**1**) and the second conducting an *O*-sulfation to generate GTX2 (**7**) and GTX3 (**8**) from a mixture of 11-α-hydroxySTX (**16**) and 11-β-hydroxySTX (**17**).[32,33] Because of enzyme instability, lack of protein sequence information, and the general intractability of manipulating dinoflagellate genomes, these enzymes were not investigated further but provided the first piece of direct evidence that sulfotransferases are critical to gonyautoxin biosynthesis. Neilan and co-workers subsequently identified the genes encoding the enzymes involved in gonyautoxin biosynthesis in cyanobacteria and proposed that they are located within the biosynthetic gene cluster for the parent compound STX (**1**), naming them SxtN and SxtSUL,[34−37] and have specifically implicated SxtN from the cyanobacteria *Syctonema crispum* as the catalyst for the conversion of STX (**1**) to gonyautoxin 5 (GTX5, **10**).[36]

To interrogate the process of PST sulfation in cyanobacteria and elucidate the biosynthetic pathway toward the C-toxins (**12−15**), we have biochemically characterized the enzymes responsible for the installation of sulfo groups *in vitro*. Toward this aim, we expressed and purified the *O*-sulfotransferase SxtSUL from *Microseira wollei* and the *N*-sulfotransferase SxtN from *Aphanizomenon* sp. NH-5 and assessed their activities on a range of substrates. Using cascade reactions with SxtSUL, SxtN, and the previously characterized Rieske oxygenase GxtA,[23] we have determined the cyanobacterial pathway

DOI: 10.1021/acschembio.9b00123
ACS Chem. Biol. 2019, 14, 941−948

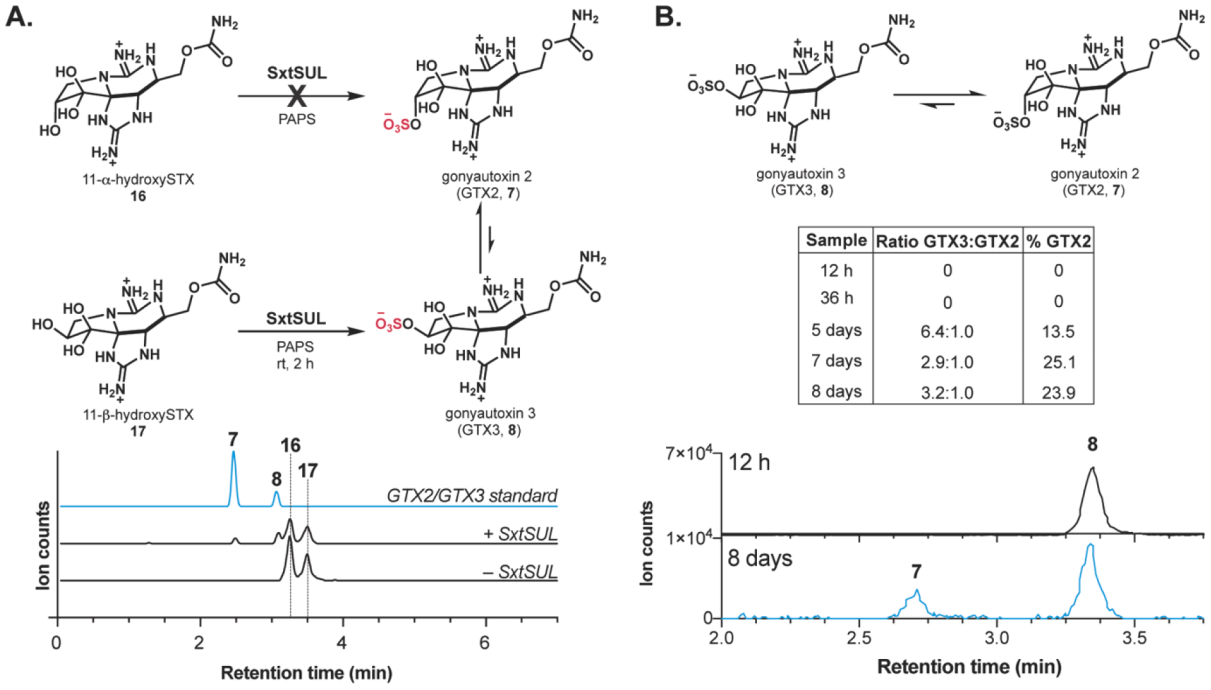

Sample	Ratio GTX3:GTX2	% GTX2
12 h	0	0
36 h	0	0
5 days	6.4:1.0	13.5
7 days	2.9:1.0	25.1
8 days	3.2:1.0	23.9

Figure 2. (A) Reaction of SxtSUL with a mixture of 11-α-hydroxySTX (**16**) and 11-β-hydroxySTX (**17**). (B) Observed epimerization of GTX3 (**8**) to GTX2 (**7**) over time.

toward GTXs, M-toxins, and C-toxins. Beyond *in vitro* characterization of C-toxin biosynthesis, we aim to demonstrate the impact of sulfation of PSTs on binding affinity to VGSCs present in mouse brain extracts. PST toxicities have been evaluated for decades using a myriad of methods including *in vivo* mouse toxicity assays, mouse or rat whole brain homogenate binding assays, and electrophysiological recordings with squid axon model systems or VGSCs in heterologous expression systems such as human embryonic kidney (HEK) or Chinese hamster ovary (CHO) cells.[38−48] For example, studies with heterologously expressed VGSCs indicate that GTX2 (**7**) and GTX3 (**8**) are comparable in toxicity to STX (**1**),[43] while squid axon studies demonstrate that GTX2 (**7**) and GTX3 (**8**) are significantly lower in toxicity relative to STX (**1**, Figure 1).[45] While there are many ways to assess toxicity, it is accepted that binding affinity of PSTs to VGSCs directly correlates with toxicity.[42,49] We aim to understand the structure activity relationships associated with PST sulfation using the reliable [^{3}H]-STX competition binding assay with mouse whole brain membrane preparations containing VGSCs in a physiologically relevant environment in order to directly compare the binding affinities of monosulfated, disulfated, and nonsulfated PSTs.[39]

RESULTS AND DISCUSSION

Characterization of SxtSUL as an *O*-Sulfotransferase. To interrogate the biosynthetic route to highly functionalized PSTs, we sought to identify the chemical functions and substrate scopes of SxtSUL and SxtN as well as the sequence of enzymatic reactions that lead to the various gonyautoxins and C-toxins. SxtSUL is proposed to be an *O*-sulfotransferase and the only characterized *O*-sulfated PST derivatives possess sulfate groups at the C11 position, as observed in GTX1−GTX4 (**6**−**9**) and C1−C4 (**12**−**15**). Thus, we sought to assess the activity of SxtSUL using a mixture of 11-α-hydroxySTX (**16**) and 11-β-hydroxySTX (**17**), putative precursors to GTX1 (**6**) and GTX2 (**7**), and GTX3 (**8**) and GTX4 (**9**), respectively. Initially, we found soluble expression and subsequent purification of SxtSUL to be challenging. We determined that coexpression of GroEL and GroES chaperone proteins with SxtSUL in a standard BL21(DE3) expression cell line was necessary to obtain sufficient quantities of soluble protein (see Supporting Information).[50] BLAST analysis indicated the presence of a conserved 3′-phosphoadenosine-5′-phosphosulfate (PAPS) binding site; thus, PAPS was employed as the sulfate donor in these reactions.[51] In analytical assays with a mixture 11-α-hydroxySTX (**16**) and 11-β-hydroxySTX (**17**), SxtSUL preferentially converted 11-β-hydroxySTX (**17**) to GTX3 (**8**, Figure 2A). However, a small amount of GTX2 (**7**) was observed in the reaction mixture, which could arise through two distinct pathways, either direct sulfation of 11-α-hydroxySTX (**16**) or from epimerization of GTX3 (**8**) to GTX2 (**7**), a phenomenon reported in the total synthesis of GTX2 (**7**) and GTX3 (**8**) by Du Bois and co-workers.[18]

To determine the operative route to GTX2 (**7**), we conducted a cascade reaction with SxtSUL and the recently characterized Rieske oxygenase, GxtA, responsible for the stereoselective conversion of STX (**1**) to 11-β-hydroxySTX (**17**).[23] This approach allowed for exclusive analysis of the epimerization pathway by generating 11-β-hydroxySTX (**17**) in situ. At early time points, we observed production of only GTX3 (**8**), which epimerized to GTX2 (**7**) over time. After 8 days of incubation at 30 °C, a 3:1 mixture of GTX3 (**8**) and GTX2 (**7**) was present (Figure 2B). Precipitation was also evident based on the decrease in ion counts over time. Additionally, the epimerization of 11-β-hydroxySTX (**17**) to 11-α-hydroxySTX (**16**) was not observed (Supporting Information Figure S7). The formation of GTX2 (**7**) and GTX3 (**8**) from a single hydroxylated precursor, 11-β-hydroxySTX (**17**), is also supported by (1) the absence of genes for GxtA homologues that would be capable of

DOI: 10.1021/acschembio.9b00123
ACS Chem. Biol. 2019, 14, 941−948

producing 11-α-hydroxySTX (**16**), (2) the absence of genes for SxtSUL homologues to react with 11-α-hydroxySTX (**16**), and (3) the absence of 11-α-hydroxySTX (**16**) in natural product extracts. These data indicate that only one *O*-sulfotransferase, SxtSUL, is required to generate GTX1−GTX4 (**6**−**9**) from 11-β-hydroxylated precursors. The enzyme required for N1 hydroxylation and the order of events in the biosynthesis of GTX1 (**6**) and GTX4 (**9**) are not known.

Substrate Scope of SxtN. Analysis of *in vitro* reactions indicated that SxtSUL performed only a single sulfation, thus a second sulfotransferase is required to introduce the sulfate onto the nitrogen atom appended to the carbamate group of the PST scaffold to afford disulfated C-toxins (**12**-**15**). Neilan and co-workers recently demonstrated that SxtN from *Syctonema crispum* can install the sulfo group onto the carbamate of STX (**1**), generating GTX5 (**10**).[36] However, the ability of SxtN to act on a broad panel of PSTs or to perform *O*-sulfations on 11-α-hydroxySTX (**16**) or 11-β-hydroxySTX (**17**) to generate GTX2 (**7**) or GTX3 (**8**) has not been assessed. Our initial experiments with heterologously expressed SxtN were conducted in vitro with STX (**1**), neoSTX (**2**), a mixture of 11-α-hydroxySTX (**16**) and 11-β-hydroxySTX (**17**), GTX2 (**7**) and GTX3 (**8**), dideoxysaxitoxin (ddSTX, **18**), α-saxitoxinol (α-STOH, **20**), and β-saxitoxinol (β-STOH, **19**). While reaction with neoSTX (**2**) and GTX2 (**7**) and GTX3 (**8**) did not result in product formation, STX (**1**) was converted to a single product, GTX5 (**10**) (Supporting Information Figure S3). Additionally, 11-α-hydroxySTX (**16**) and 11-β-hydroxySTX (**17**) were not observably sulfamated by SxtN, definitively demonstrating that SxtN exclusively acts as a *N*-sulfotransferase. Interestingly, reactions with substrates at a lower oxidation level than STX (**1**) such as ddSTX (**18**), α-STOH (**20**), and β-STOH (**19**) resulted in the formation of sulfonated products in each case (Figure 3). Relative percent conversions were assessed for each of these transformations by LC-MS and suggest that STX (**1**) is the preferred substrate of SxtN (Supporting Information Figure S3). Steady-state kinetic analysis of SxtN with STX (**1**) revealed a k_{cat}/K_M of 0.44 M s^{-1} (Figure 3). K_M values greater than 1 mM were observed with α-STOH (**20**) and β-STOH (**19**) (Supporting Information Figure S5). Additionally, steady-state kinetic analysis of PAPS using constant saturating STX (**1**) revealed a K_M of 6.2 ± 1.4 μM, a value consistent with other characterized PAPS-dependent sulfotransferases (Figure 3).[52]

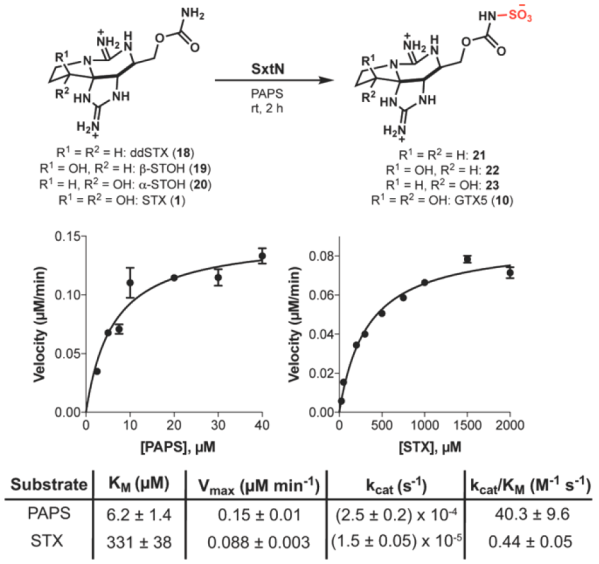

Substrate	K_M (μM)	V_{max} (μM min^{-1})	k_{cat} (s^{-1})	k_{cat}/K_M (M^{-1} s^{-1})
PAPS	6.2 ± 1.4	0.15 ± 0.01	(2.5 ± 0.2) x 10^{-4}	40.3 ± 9.6
STX	331 ± 38	0.088 ± 0.003	(1.5 ± 0.05) x 10^{-5}	0.44 ± 0.05

Figure 3. SxtN reactions with non-native substrates and steady-state kinetics with PAPS and STX (**1**).

***In Vitro* Enzyme Cascades.** To determine the order of events leading to toxins C1 (**12**) and C2 (**13**), we conducted cascade reactions with SxtN, GxtA, and SxtSUL using STX (**1**) as a substrate. As SxtN was only capable of reacting with substrates at or below the STX (**1**) oxidation state, we hypothesized that SxtN must react with STX (**1**) before GxtA hydroxylation and SxtSUL installation of the C11 sulfate group. In reactions containing only SxtN and GxtA, the emergence of a new product with the exact mass of GTX2 (**7**) and GTX3 (**8**), m/z = 396, and higher polarity than GTX5 (**10**) was observed by hydrophilic interaction liquid chromatography (HILIC)-MS (Figure 4B). By MS/MS analysis, this new product corresponded to hydroxylated GTX5, a natural product toxin previously isolated and named M1, consisting of epimers M1α (**3**) and M1β (**4**).[4,53] The retention time and MS/MS fragmentation pattern differed from GTX3 (**8**) with the enhanced fragmentation peak at 316 suggested the cleavage of the sulfocarbamate with a remaining C11 hydroxylated tricycle (Supporting Information Figure S10). This fragmentation pattern was also observed in the reported MS/MS spectrum of M1 epimers.[4] Furthermore, the addition of SxtSUL to a reaction containing SxtN and GxtA resulted in the formation of GTX3 (**8**) and toxin C2 (**13**, Figure 4C), confirming the identity of the M1 epimer produced by SxtN and GxtA to be M1β (**4**). The identity of toxin C2 (**13**) was verified using an authentic standard by LC-MS (Figure 4C). Collectively, these experiments represent the first direct characterization of the biosynthetic enzymes and relevant biosynthetic intermediates necessary for the generation of M-toxins the disulfated C-toxins from STX (**1**) in cyanobacteria, demonstrating an imperative order of events.

Affinity for Voltage-Gated Sodium Channels. Previous *in vitro* work using a high-throughput 96-well [^{3}H]-STX binding assay developed by Usup and co-workers reported the monosulfated PSTs to have a reduced affinity compared to STX (**1**) and neoSTX (**2**) for the tetrodotoxin-sensitive VGSCs present in rat brain preparations.[42] *In vivo* work using the mouse toxicity assay also indicated the sulfated PSTs have reduced toxicity compared to STX (**1**) and neoSTX (**2**).[54] To pharmacologically characterize the therapeutic potential of the PSTs explored in this study and assess relative toxicity, competitive [^{3}H]-STX binding assays using mouse whole brain membrane preparations were performed.[39]

Competitive binding curves for the unlabeled toxins against 5 nM [^{3}H]-STX are shown in Figure 5. The relative K_i values for each unlabeled toxin are shown in Figure 5. K_i values ranged from 0.875 to 625.2 nM for STX (**1**) and a mixture of toxins C1 (**12**) and C2 (**13**), respectively. The competitive binding curves for GTX2 (**7**) and GTX3 (**8**), 11-α-hydroxySTX (**16**) and 11-β-hydroxySTX (**17**), GTX5 (**10**), and toxins C1 (**12**) and C2 (**13**) were shifted to the right of unlabeled STX (**1**), indicating a lower affinity than STX (**1**) for the VGSCs present in the mouse whole-brain preparations. The rank order of binding affinity according to K_i values was STX (**1**) > GTX2/3 (**7**, **8**) > 11-α/β-hydroxySTX (**16**, **17**) > GTX5 (**10**) > C1/C2 (**12**, **13**). At 10 μM, each of the unlabeled toxins displaced more than 92% of the [^{3}H]-STX

DOI: 10.1021/acschembio.9b00123
ACS Chem. Biol. 2019, 14, 941−948

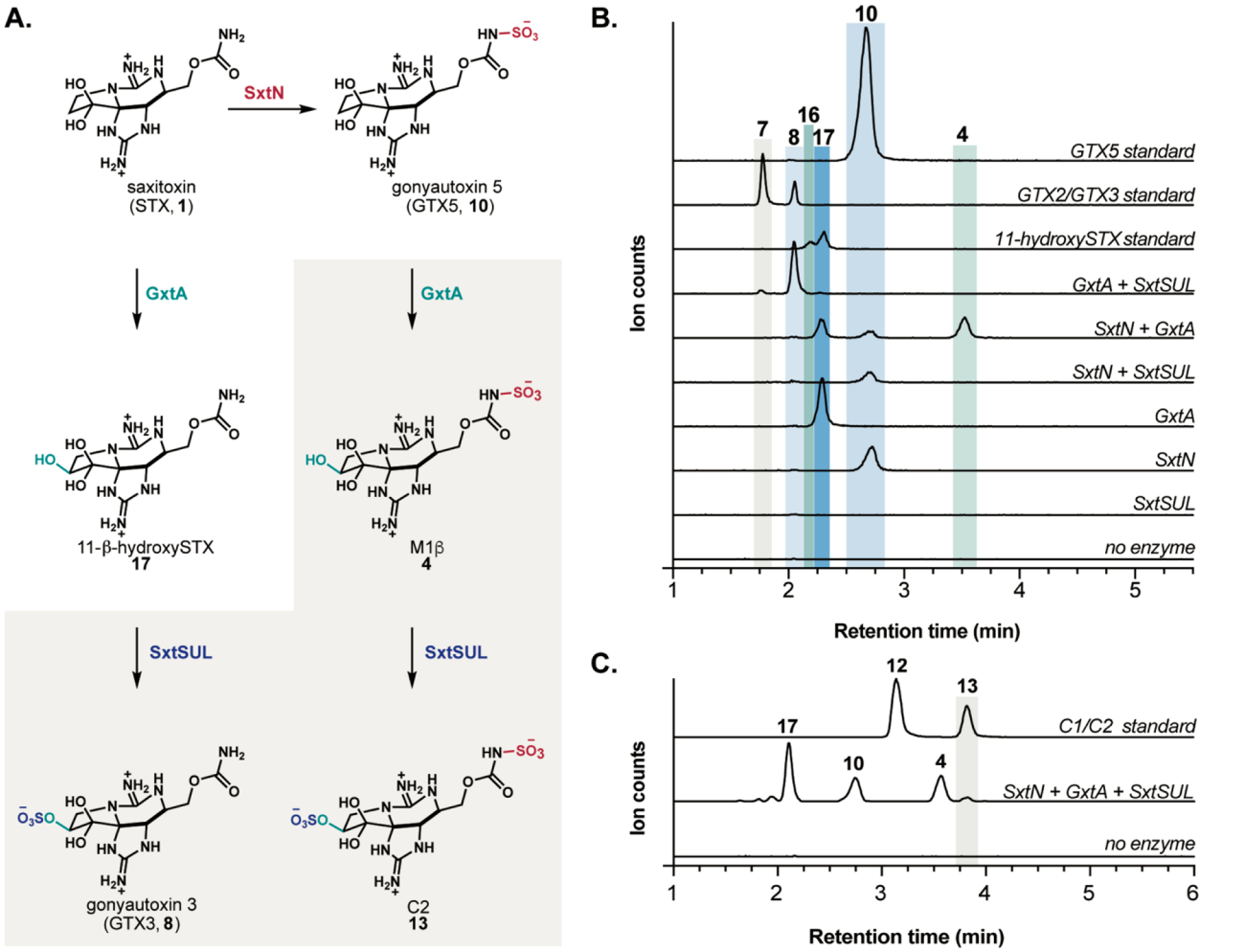

Figure 4. Cascade reactions with SxtN, GxtA, and SxtSUL. (A) Scheme of cascade reactions en route to natural products boxed in gray. (B) LC-MS traces of one and two enzyme reactions compared to product standards. (C) LC-MS traces of SxtN + GxtA + SxtSUL reaction compared to C1 (**12**) and C2 (**13**) product standard.

present, except the mixture of C1 (**12**) and C2 (**13**), which only reached ~80% total displacement of [^{3}H]-STX. The curves for GTX2/3 (**7**, **8**) and 11-α/β-hydroxySTX (**16**, **17**) clustered together, signifying similar VGSC affinity. However, the K_i of GTX5 (**10**) was roughly 2-fold higher than these toxins and the K_i measured for the mixture of C1 (**12**) and C2 (**13**) was over 10-fold higher, indicating a more significant role in VGSC binding affinity for the negatively charged sulfate appended to the nitrogen of the carbamate than the C11 position.

In light of recent structural studies demonstrating binding interactions of STX (**1**) with the pore of the insect VGSC, Na_vPaS, it is now known that the amine of the carbamate of STX (**1**) forms a key hydrogen bond with the side chain of Gln1062.[55] Similar H-bond donating residues are not reported within the vicinity of the C11 position. These observations correlate with the results of a study by Du Bois and co-workers assessing different functional groups at the carbamate position of STX (**1**), where the addition of steric bulk did not reduce the molecule's VGSC potency unless the group was negatively charged.[56] Thus, the reduction in affinity observed with sulfocarbamate-containing PSTs compared to C11-sulfated PSTs in our study is corroborated by structural information. These data suggest the importance of considering bulky, negatively charged functional groups in the design of safer, lower toxicity PST analogs as therapeutics.

Conclusions. In summary, we have elucidated the biosynthetic steps necessary to achieve GTX2 (**7**), GTX3 (**8**), M1β (**4**), and C2 (**13**) from STX (**1**) using individual and cascade reactions with the sulfotransferases SxtN and SxtSUL and oxygenase GxtA. We have also directly demonstrated the detoxification effect of further modifications to the STX (**1**) scaffold by sulfation using competitive [^{3}H]-STX displacement assays in mouse whole brain. This work sheds light on the remarkable biological processes regulating PST toxicity in cyanobacteria. The characterized enzymes herein have the potential to become powerful biocatalytic tools for producing sulfated PSTs, empowering the study of VGSC biology and the development of therapeutics for VGSC disorders.

METHODS

Protein Expression and Purification. GxtA and VanB were expressed and purified as described previously.[23] A pMCSG7 expression vector containing *sxtSUL* was transformed into the *E. coli* BL21(DE3) containing the pGro7 plasmid for the coexpression of GroEL and GroES chaperones, and a pMCSG7 vector containing sxtN was transformed into BL21(DE3) only. All proteins were purified using a GE Healthcare ÄKTA Pure FPLC with 5 mL of HisTrap, 5 mL of MBPTrap, or HiPrep 16/60 Sephacryl S-200 high-

DOI: 10.1021/acschembio.9b00123
ACS Chem. Biol. 2019, 14, 941−948

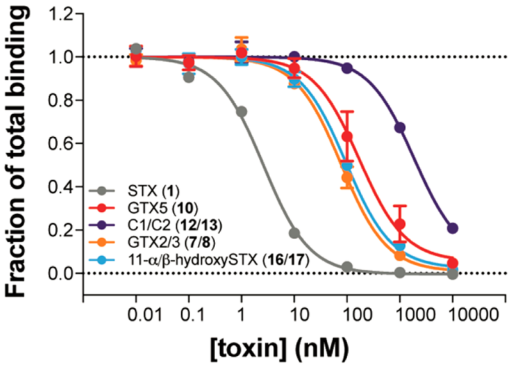

Compound	K_i (nM)	95% confidence interval
STX (**1**)	0.8756	0.6731 to 1.142
GTX5 (**10**)	56.98	30.98 to 109.8
11-α/β-hydroxySTX (**16/17**)	31.89	23.91 to 42.4
GTX2/3 (**7/8**)	25.94	18.89 to 35.32
C1/C2 (**12/13**)	625.2	441.8 to 913.3

Figure 5. Concentration response curves showing specific binding of PSTs to mouse whole-brain membrane samples in competition with 5 nM [^{3}H]-saxitoxin. K_i values listed are determined from concentration response curves.

resolution columns (GE Healthcare) using conditions described in detail in the Supporting Information Appendix. Purified proteins were frozen in liquid nitrogen and stored at −80 °C. Proteins were discarded after one freeze−thaw cycle.

Enzymatic Reactions and Analysis. All reactions were performed on analytical scale in 50 μL volumes prepared in 1.5 mL plastic centrifuge tubes. For reactions containing individual enzymes, 5 μM SxtSUL or SxtN was combined with 200 μM of substrate (STX (**1**) for SxtN and a mixture of 11-α-hydroxySTX (**16**) and 11-β-hydroxySTX (**17**) for SxtSUL), 100 μM PAPS, and 50 mM HEPES pH 7.0 buffer. Reactions were incubated at RT (22 °C) for 2 h without agitation. Cascade reactions containing multiple enzymes were performed by combining 20 μM SxtSUL, 20 μM SxtN, 5 μM GxtA, 5 μM VanB, 200 μM STX (**1**), 200 μM PAPS, 500 μM NADH, 100 μM $Fe(NH_4)_2(SO_4)_2$, and 50 mM TrisHCl pH 7.0 buffer. Reactions were incubated at RT overnight (∼10 h) without agitation. All reactions were quenched by the addition of 3× volume HPLC-grade acetonitrile (150 μL) and centrifuged at 12,000×*g* for 20 min. For LC-MS analysis, 100 μL of the supernatant was diluted with a mixture of 50% v/v acetonitrile and 50% v/v sterile-filtered ddH_2O containing 1% v/v formic acid and 6 μg mL^{-1} ^{15}N-arginine as an internal standard. All separations were performed using an Acquity UPLC BEH Amide 1.7 μm, 2.1 × 100 mm hydrophobic interaction liquid chromatography (HILIC) column from Waters with an isocratic mobile phase of 18% water with 0.1% formic acid and 82% of 95% acetonitrile, 5% water and 0.1% formic acid (v/v) at 0.4 mL min^{-1}.

Mouse Whole Brain Binding Assays. Whole brain membranes were prepared from adult (postnatal day (P) 30−150) wildtype C57Bl/6J mice as described previously.[39] Equilibrium [^{3}H]-STX binding in the presence or absence of PST was measured at 4 °C for at least 1 h using a vacuum filtration assay with a saturating concentration (5 nM) C11 labeled [^{3}H]-STX (20 Ci mmol^{-1}, American Radiolabeled Chemicals Inc.). A stock of each unlabeled toxin was diluted in binding buffer to give a final concentration of 10 000, 1000, 100, 10, 1, 0.1, and 0.01 nM. A 7-point concentration−response curve was generated for each unlabeled PST in competition with 5 nM [^{3}H]-STX. Two independent experiments were conducted for each unlabeled PST, and in each experiment each sample was tested in duplicate. The average DPM reading of duplicate values was used for analysis.

Synthesis and Standard Preparation. Product standards of ddSTX (**18**), α-STOH (**20**), β-STOH (**19**), STX (**1**), neoSTX (**2**), 11-α-hydroxySTX (**16**), 11-β-hydroxySTX (**17**), GTX2 (**7**), and GTX3 (**8**) were prepared as previously described.[23] GTX5 (**10**), C1 (**12**), and C2 (**13**) were authentic standards purchased from National Research Council Canada.

■ ASSOCIATED CONTENT

Supporting Information

The Supporting Information is available free of charge on the ACS Publications website at DOI: 10.1021/acschembio.9b00123.

Supplemental figures and methods (PDF)

■ AUTHOR INFORMATION

Corresponding Author

*E-mail: arhardin@umich.edu.

ORCID

Nicholas Denomme: 0000-0002-7631-0385

Alison R. H. Narayan: 0000-0001-8290-0077

Notes

The authors declare no competing financial interest.

■ ACKNOWLEDGMENTS

This research was supported by funds from the University of Michigan Life Sciences Institute and the National Institute of General Medical Science R35GM124880 (to A.R.H.N.) and the National Institute of Neurological Disorders and Stroke R37NS076752 (to L.L.I.). We thank D. Ellinwood for assistance with synthesis and J. Iñiguez-Lluhí for helpful discussions.

■ REFERENCES

(1) Llewellyn, L. E. (2006) Saxitoxin, a toxic marine natural product that targets a multitude of receptors. *Nat. Prod. Rep. 23*, 200−222.

(2) Thottumkara, A. P., Parsons, W. H., and Du Bois, J. (2014) Saxitoxin. *Angew. Chem., Int. Ed. 53*, 5760−5784.

(3) Robertson, A., Negri, A. P., Burnell, J. N., and Llewellyn, L. E. (2006) Development and assessment of radioreceptor binding assays for the detection of saxitoxin binding proteins in biological extracts. *Anal. Biochem. 356*, 66−75.

(4) Dell' Aversano, C., Walter, J. A., Burton, I. W., Stirling, D. J., Fattorusso, E., and Quilliam, M. A. (2008) Isolation and structure elucidation of new and unusual saxitoxin analogues from mussels. *J. Nat. Prod. 71*, 1518−1523.

(5) Laycock, M. V., Kralovec, J., and Richards, R. (1997) A simple procedure for sulfation and ^{35}S radiolabelling of paralytic shellfish poisoning (PSP) gonyautoxins. *Nat. Toxins 5*, 36−42.

(6) van Apeldoorn, M. E., van Egmond, H. P., Speijers, G. J. A., and Bakker, G. J. I. (2007) Toxins of cyanobacteria. *Mol. Nutr. Food Res. 51*, 7−60.

(7) Bustillos-Guzman, J. J., Band-Schmidt, C. J., Duran-Riveroll, L. M., Hernandez-Sandoval, F. E., Lopez-Cortes, D. J., Nunez-Vazquez, E. J., Cembella, A., and Krock, B. (2015) Paralytic toxin profile of the marine dinoflagellate *Gymnodinium catenatum Graham* from the Mexican Pacific as revealed by LC-MS/MS. *Food Addit. Contam., Part A 32*, 1−14.

(8) Andrinolo, D., Michea, L. F., and Lagos, N. (1999) Toxic effects, pharmacokinetics and clearance of saxitoxin, a component of paralytic shellfish poison (PSP), in cats. *Toxicon 37*, 447−464.

(9) Andrinolo, D., Iglesias, V., Garcia, C., and Lagos, N. (2002) Toxicokinetics and toxicodynamics of gonyautoxins after an oral toxin dose in cats. *Toxicon 40*, 699−709.

(10) Lattes, K., Venegas, P., Lagos, N., Lagos, M., Pedraza, L., Rodriguez-Navarro, A. J., and Garcia, C. (2009) Local infiltration of

DOI: 10.1021/acschembio.9b00123
ACS Chem. Biol. 2019, 14, 941−948

gonyautoxin is safe and effective in treatment of chronic tension-type headache. *Neurol. Res. 31*, 228−33.
(11) Garrido, R., Lagos, N., Lattes, K., Abedrapo, M., Bocic, G., Cuneo, A., Chiong, H., Jensen, C., Azolas, R., Henriquez, A., and Garcia, C. (2005) Gonyautoxin: New treatment for healing acute and chronic anal fissures. *Dis. Colon Rectum 48*, 335−340.
(12) Garrido, R., Lagos, N., Lagos, M., Rodriguez-Navarro, A. J., Garcia, C., Truan, D., and Henriquez, A. (2007) Treatment of chronic anal fissure by gonyautoxin. *Colorectal Dis. 9*, 619−624.
(13) Hinzpeter, J., Barrientos, C., Zamorano, A., Martinez, A., Palet, M., Wulf, R., Barahona, M., Sepulveda, J. M., Guerra, M., Bustamante, T., Del Campo, M., Tapia, E., and Lagos, N. (2016) Gonyautoxins: First evidence in pain management in total knee arthroplasty. *Toxicon 119*, 180−185.
(14) Naumann, M., So, Y., Argoff, C. E., Childers, M. K., Dykstra, D. D., Gronseth, G. S., Jabbari, B., Kaufmann, H. C., Schurch, B., Silberstein, S. D., and Simpson, D. M. (2008) Assessment: Botulinum neurotoxin in the treatment of autonomic disorders and pain (an evidence-based review) - Report of the Therapeutics and Technology Assessment Subcommittee of the American Academy of Neurology. *Neurology 70*, 1707−1714.
(15) Mueller, C., Altenburger, U., and Mohl, S. (2018) Challenges for the pharmaceutical technical development of protein coformulations. *J. Pharm. Pharmacol. 70*, 666−674.
(16) Frokjaer, S., and Otzen, D. E. (2005) Protein drug stability: A formulation challenge. *Nat. Rev. Drug Discovery 4*, 298−306.
(17) Fleming, J. J., and Du Bois, J. (2006) A synthesis of (+)-saxitoxin. *J. Am. Chem. Soc. 128*, 3926.
(18) Mulcahy, J. V., Walker, J. R., Merit, J. E., Whitehead, A., and Du Bois, J. (2016) Synthesis of the paralytic shellfish poisons (+)-gonyautoxin 2, (+)-gonyautoxin 3, and (+)-11,11-dihydroxysaxitoxin. *J. Am. Chem. Soc. 138*, 5994−6001.
(19) Sawayama, Y., and Nishikawa, T. (2012) A new synthetic route to the skeleton of saxitoxin, a naturally occurring blocker of voltage-gated sodium channels. *J. Synth. Org. Chem., Jpn. 70*, 1178−1186.
(20) Ueno, S., Nakazaki, A., and Nishikawa, T. (2016) A synthetic strategy for saxitoxin skeleton by a cascade bromocyclization: Total synthesis of (+)-decarbamoyl-alpha-saxitoxinol. *Org. Lett. 18*, 6368−6371.
(21) Garrido, R., Lagos, N., Lattes, K., Garcia, C., Azolas, R., Bocic, G., Cuneo, A., Chiong, H., Jensen, C., Henriquez, A., and Fernandez, C. (2004) The Gonyautoxin 2/3 epimers reduces anal tone when injected in the anal sphincter of healthy adults. *Biol. Res. 37*, 395−403.
(22) Chun, S. W., Hinze, M. E., Skiba, M. A., and Narayan, A. R. H. (2018) Chemistry of a unique polyketide-like synthase. *J. Am. Chem. Soc. 140*, 2430−2433.
(23) Lukowski, A. L., Ellinwood, D. C., Hinze, M. E., DeLuca, R. J., Du Bois, J., Hall, S., and Narayan, A. R. H. (2018) C−H hydroxylation in paralytic shellfish toxin biosynthesis. *J. Am. Chem. Soc. 140*, 11863−11869.
(24) Vasama, M., Kumar, H., Salminen, S., and Haskard, C. A. (2014) Removal of paralytic shellfish toxins by probiotic lactic acid acteria. *Toxins 6*, 2127−2136.
(25) Donovan, C. J., Ku, J. C., Quilliam, M. A., and Gill, T. A. (2008) Bacterial degradation of paralytic shellfish toxins. *Toxicon 52*, 91−100.
(26) Fabioux, C., Sulistiyani, Y., Haberkorn, H., Hegaret, H., Amzil, Z., and Soudant, P. (2015) Exposure to toxic *Alexandrium minutum* activates the detoxifying and antioxidant systems in gills of the oyster *Crassostrea gigas*. *Harmful Algae 48*, 55−62.
(27) Qiu, J. B., Meng, F. P., Ding, L., Che, Y. J., McCarron, P., Beach, D. G., and Li, A. F. (2018) Dynamics of paralytic shellfish toxins and their metabolites during timecourse exposure of scallops *Chlamys farreri* and mussels *Mytilus galloprovincialis* to *Alexandrium pacificum*. *Aquat. Toxicol. 200*, 233−240.
(28) Li, Y. L., Sun, X. Q., Hu, X. L., Xun, X. G., Zhang, J. B., Guo, X. M., Jiao, W. Q., Zhang, L. L., Liu, W. Z., Wang, J., Li, J., Sun, Y., Miao, Y., Zhang, X. K., Cheng, T. R., Xu, G. L., Fu, X. T., Wang, Y. F., Yu, X. R., Huang, X. T., Lu, W., Lv, J., Mu, C., Wang, D. W., Li, X., Xia, Y., Li, Y. J., Yang, Z. H., Wang, F. L., Zhang, L., Xing, Q., Dou, H. Q., Ning, X. H., Dou, J. Z., Li, Y. P., Kong, D. X., Liu, Y. R., Jiang, Z., Li, R. Q., Wang, S., and Bao, Z. M. (2017) Scallop genome reveals molecular adaptations to semi−sessile life and neurotoxins. *Nat. Commun. 8*, 11.
(29) Van Egmond, H. P., Jonker, K. M., Poelman, M., Scherpenisse, P., Stern, A. G., Wezenbeek, P., Bergwerff, A. A., and Van den Top, H. J. (2004) Proficiency studies on the determination of paralytic shellfish poisoning toxins in shellfish. *Food Addit. Contam. 21*, 331−340.
(30) Jellett, J. F., Stewart, J. E., and Laycock, M. V. (1995) Toxicological evaluation of saxitoxin, neosaxitoxin, gonyautoxin-II, gonyautoxin-II-+-III and decarbamoylsaxitoxin with the mouse neuroblastoma cell bioassay. *Toxicol. In Vitro 9*, 57−65.
(31) Soto-Liebe, K., Murillo, A. A., Krock, B., Stucken, K., Fuentes-Valdes, J. J., Trefault, N., Cembella, A., and Vasquez, M. (2010) Reassessment of the toxin profile of *Cylindrospermopsis raciborskii* T3 and function of putative sulfotransferases in synthesis of sulfated and sulfonated PSP toxins. *Toxicon 56*, 1350−1361.
(32) Sako, Y., Yoshida, T., Uchida, A., Arakawa, O., Noguchi, T., and Ishida, Y. (2001) Purification and characterization of a sulfotransferase specific to N-21 of saxitoxin and gonyautoxin 2 + 3 from the toxic dinoflagellate *Gymnodinium catenatum* (Dinophyceae). *J. Phycol. 37*, 1044−1051.
(33) Yoshida, T., Sako, Y., Uchida, A., Kakutani, T., Arakawa, O., Noguchi, T., and Ishida, Y. (2002) Purification and characterization of sulfotransferase specific to O-22 of 11-hydroxysaxitoxin from the toxic dinoflagellate *Gymnodinium catenatum* (Dinophyceae). *Fish. Sci. 68*, 634−642.
(34) Kellmann, R., Mihali, T. K., Jeon, Y. J., Pickford, R., Pomati, F., and Neilan, B. A. (2008) Biosynthetic intermediate analysis and functional homology reveal a saxitoxin gene cluster in cyanobacteria. *Appl. Environ. Microbiol. 74*, 4044−4053.
(35) Mihali, T. K., Kellmann, R., and Neilan, B. A. (2009) Characterisation of the paralytic shellfish toxin biosynthesis gene clusters in *Anabaena circinalis* AWQC131C and *Aphanizomenon* sp. NH-5. *BMC Biochem. 10*, 8.
(36) Cullen, A., D'Agostino, P. M., Mazmouz, R., Pickford, R., Wood, S., and Neilan, B. A. (2018) Insertions within the saxitoxin biosynthetic gene cluster result in differential toxin profiles. *ACS Chem. Biol. 13*, 3107−3114.
(37) Mihali, T. K., Carmichael, W. W., and Neilan, B. A. (2011) A putative gene cluster from a *Lyngbya wollei* bloom that encodes paralytic shellfish toxin biosynthesis. *PLoS One 6*, No. e14657.
(38) Jellett, J. F., Marks, L. J., Stewart, J. E., Dorey, M. L., Watsonwright, W., and Lawrence, J. F. (1992) Paralytic shellfish poison (saxitoxin family) bioassays - automated end-point determination and standardization of the *in vitro* tissue-culture bioassay, and comparison with the standard mouse bioassay. *Toxicon 30*, 1143−1156.
(39) Isom, L. L., Scheuer, T., Brownstein, A. B., Ragsdale, D. S., Murphy, B. J., and Catterall, W. A. (1995) Functional co−expression of the β1 and Type IIA α subunits of sodium channels in a mammalian cell line. *J. Biol. Chem. 270*, 3306−3312.
(40) Tsukamoto, T., Chiba, Y., Wakamori, M., Yamada, T., Tsunogae, S., Cho, Y., Sakakibara, R., Imazu, T., Tokoro, S., Satake, Y., Adachi, M., Nishikawa, T., Yotsu-Yamashita, M., and Konoki, K. (2017) Differential binding of tetrodotoxin and its derivatives to voltage-sensitive sodium channel subtypes (Na_v 1.1 to Na_v 1.7). *Br. J. Pharmacol. 174*, 3881−3892.
(41) Walker, J. R., Novick, P. A., Parsons, W. H., McGregor, M., Zablocki, J., Pande, V. S., and Du Bois, J. (2012) Marked difference in saxitoxin and tetrodoxin affinity for the human nociceptive voltage-gated sodium channel (Na_v1.7). *Proc. Natl. Acad. Sci. U. S. A. 109*, 18102.
(42) Usup, G., Leaw, C., Cheah, M., Ahmad, A., and Ng, B. (2004) Analysis of paralytic shellfish poisoning toxin congeners by a sodium channel receptor binding assay. *Toxicon 44*, 37−43.

DOI: 10.1021/acschembio.9b00123
ACS Chem. Biol. 2019, 14, 941−948

(43) Alonso, E., Alfonso, A., Vieytes, M. R., and Botana, L. M. (2016) Evaluation of toxicity equivalent factors of paralytic shellfish poisoning toxins in seven human sodium channels types by an automated high throughput electrophysiology system. *Arch. Toxicol. 90*, 479−488.
(44) Hall, S., Strichartz, G., Moczydlowski, E., Ravindran, A., and Reichardt, P. B. (1990) The saxitoxins - sources, chemistry, and pharmacology. *ACS Symp. Ser. 418*, 29−65.
(45) Kao, C. Y., Kao, P. N., James-Krace, M. R., Koehn, F. E., Wichmann, C. F., and Schnoes, H. K. (1985) Actions of epimers of 12-(OH)-reduced saxitoxin and of 11-(OSO_3)-saxitoxin on squid axon. *Toxicon 23* (4), 647−655.
(46) Genenah, A. A., and Shimizu, Y. (1981) Specific toxicity of paralytic shellfish poisons. *J. Agric. Food Chem. 29* (6), 1289−1291.
(47) Hall, S. *Toxins and toxicity of Protogonyaulax from the northeast Pacific*; University of Alaska: Fairbanks, 1982.
(48) Strichartz, G., Rando, T., Hall, S., Gitschier, J., Hall, L., Magnani, B., and Bay, C. H. (1986) On the mechanism by which saxitoxin binds to and blocks sodium-channels. *Ann. N. Y. Acad. Sci. 479*, 96−112.
(49) Duran-Riveroll, L. M., and Cembella, A. D. (2017) Guanidinium toxins and their interactions with voltage-gated sodium ion channels. *Mar. Drugs 15*, 303.
(50) Nishihara, K., Kanemori, M., Kitagawa, M., Yanagi, H., and Yura, T. (1998) Chaperone coexpression plasmids: Differential and synergistic roles of DnaK-DnaJ-GrpE and GroEL-GroES in assisting folding of an allergen of Japanese cedar pollen, Cryj2 in *Escherichia coli*. *Appl. Environ. Microbiol. 64*, 1694−1699.
(51) Negishi, M., Pedersen, L. G., Petrotchenko, E., Shevtsov, S., Gorokhov, A., Kakuta, Y., and Pedersen, L. C. (2001) Structure and function of sulfotransferases. *Arch. Biochem. Biophys. 390*, 149−157.
(52) Paul, P., Suwan, J., Liu, J., Dordick, J. S., and Linhardt, R. J. (2012) Recent advances in sulfotransferase enzyme activity assays. *Anal. Bioanal. Chem. 403*, 1491−500.
(53) D'Agostino, P. M., Boundy, M. J., Harwood, T. D., Carmichael, W. W., Neilan, B. A., and Wood, S. A. (2019) Re-evaluation of paralytic shellfish toxin profiles in cyanobacteria using hydrophilic interaction liquid chromatography-tandem mass spectrometry. *Toxicon 158*, 1−7.
(54) Alexander, J., Benford, D., Cockburn, A., Cravedi, J., Dogliotti, E., Di Domenico, A., Fernández-Cruz, M., Fink-Gremmels, J., Fürst, P., Galli, C., Grandjean, P., Gzyl, J., Heinemeyer, G., Johansson, N., Mutti, A., Schlatter, J., Van Leeuwen, R., Van Peteghem, C., and Verger, P. (2009) Scientific opinion of the panel on contaminants in the food chain on a request from the European commission on marine biotoxins in shellfish — Saxitoxin group. *EFSA Journal 1019*, 1−76.
(55) Shen, H. Z., Li, Z. Q., Jiang, Y., Pan, X. J., Wu, J. P., Cristofori-Armstrong, B., Smith, J. J., Chin, Y. K. Y., Lei, J. L., Zhou, Q., King, G. F., and Yan, N. (2018) Structural basis for the modulation of voltage-gated sodium channels by animal toxins. *Science 362*, eeau2596.
(56) Andresen, B. M., and Du Bois, J. (2009) *De novo* synthesis of modified saxitoxins for sodium ion channel study. *J. Am. Chem. Soc. 131*, 12524−12525.

DOI: 10.1021/acschembio.9b00123
ACS Chem. Biol. 2019, 14, 941−948